

Margaret Harder · James K. Russell

Basanite glaciovolcanism at Llangorse mountain, northern British Columbia, Canada

Received: 26 November 2004 / Accepted: 24 March 2006 / Published online: 23 May 2006
© Springer-Verlag 2006

Abstract The Llangorse volcanic field is located in northwest British Columbia, Canada, and comprises erosional remnants of Miocene to Holocene volcanic edifices, lava flows or dykes. The focus of this study is a single overthickened, 100-m-thick-valley-filling lava flow that is Middle-Pleistocene in age and located immediately south of Llangorse Mountain. The lava flow is basanitic in composition and contains mantle-derived peridotite xenoliths. The lava directly overlies a sequence of poorly sorted, crudely bedded volcanoclastic debris-flow sediments. The debris flow deposits contain a diverse suite of clast types, including angular clasts of basanite lava, blocks of peridotite coated by basanite, and rounded boulders of granodiorite. Many of the basanite clasts have been palagonitized. The presence and abundance of clasts of vesicular to scoriaceous, palagonitized basanite and peridotite suggest that the debris flows are syngenetic to the overlying lava flow and sampled the same volcanic vent during the early stages of eruption. They may represent lahars or outburst floods related to melting of a snow pack or ice cap during the eruption. The debris flows were water-saturated when deposited. The rapid subsequent emplacement of a thick basanite flow over the sediments heated pore fluids to at least 80–100°C causing in-situ palagonitization of glassy basanite clasts within the sediments. The over-thickened nature of the Llangorse Mountain lavas suggests ponding of the lava against a down-stream barrier. The distribution of similar-aged glaciovolcanic features in the cordillera suggests the possibility that the barrier was a lower-elevation, valley-wide ice-sheet.

Keywords Glaciovolcanism · Basanite · Lahar · Palagonite · Thermal-model · British Columbia

Introduction

The Northern Cordilleran Volcanic Province (NCVP) comprises Miocene to Holocene volcanic rocks distributed across northwestern British Columbia, the Yukon Territory, and eastern Alaska (Edwards and Russell 2000). The NCVP is dominated by small, mafic alkaline centres that represent single eruptive events or cycles, although long-lived, chemically evolved volcanic centres do occur (e.g., Mount Edziza, Hoodoo Mountain, Level Mountain). Many of the volcanic edifices and remnants that comprise the NCVP display subglacial and ice-contact features, indicating that these eruptions coincided with periods of continental glaciation (e.g., Mathews 1947; Edwards et al. 2002; Edwards and Russell 2002).

The Llangorse volcanic field (LVF) is approximately 144 km² and is located approximately 55 km southeast of Atlin, British Columbia near Llangorse Mountain (Fig. 1). Here, we present field observations and petrographic descriptions for a basanite lava flow and associated volcanoclastic deposits exposed near Llangorse Mountain. This information is used to constrain the volcanological origins of these deposits. Our study of this valley-filling lava and the underlying debris flow deposits suggests that the lava and sediments result from a short-lived, synglacial volcanic eruption originating at a vent that has been subsequently removed by glaciation.

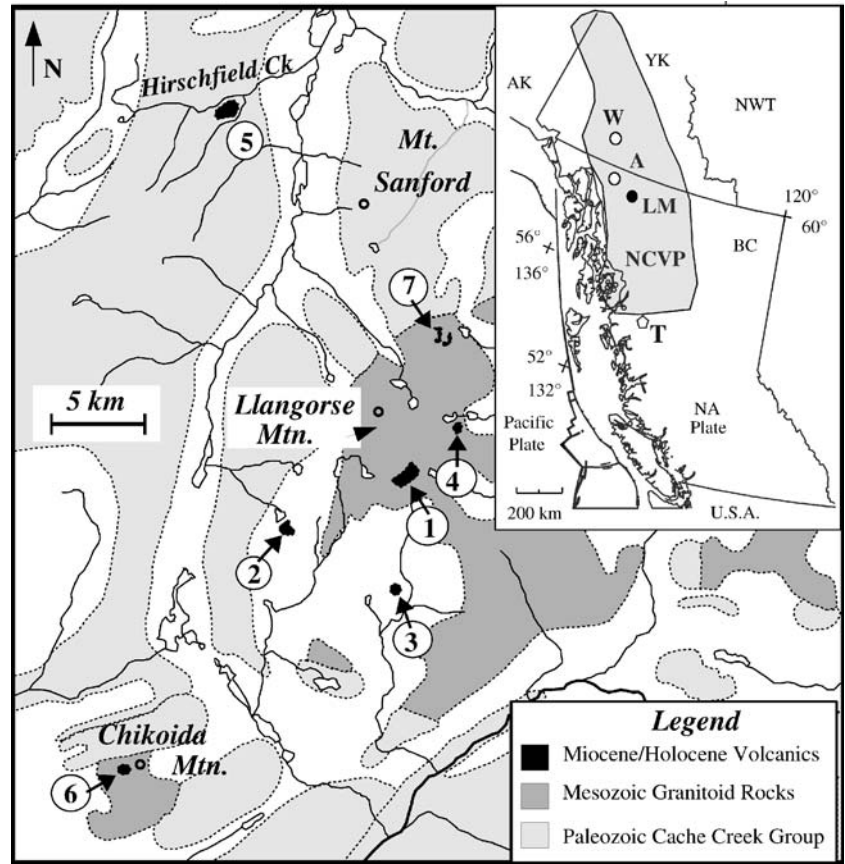
Editorial responsibility: H. Delgado

M. Harder · J. K. Russell (✉)
Volcanology & Petrology Laboratory, Earth & Ocean Sciences,
The University of British Columbia,
Vancouver, BC, V6T 1Z4, Canada
e-mail: krussell@eos.ubc.ca
Tel.: +1-604-8222703
Fax: +1-604-8226088

The Llangorse volcanic field

Aitken (1959) produced the first regional geology map for the Atlin area and reported numerous remnants of young volcanic deposits. The region lies entirely within the Intermontane Belt and is underlain by Paleozoic sedimentary and volcanoclastic rocks from the Cache Creek Group and by granitic to granodioritic plutons ranging in age from

Fig. 1 Geological map of Llangorse volcanic field (LVF; Map Sheet NTS 104N; after Aitken 1959 and Harder et al. 2003). The LVF includes occurrences of Miocene–Holocene volcanic rocks (Table 1) at: 1 Llangorse Mountain, 2 Table Hill, 3 Lone Point, 4 Hidden Ridge, 5 Hirschfeld Creek, 6 Chikoida Mountain, and 7 Fire Mountain. *Inset* shows the northern Cordilleran volcanic province (NCVP; shaded area) comprising Miocene–Holocene volcanic centres within northern British Columbia (BC), the Yukon territory (YK) and easternmost Alaska (AK) (Edwards and Russell 2000). Geographic reference points include Whitehorse (W), Atlin (A), Terrace (T) and Llangorse Mountain (LM)



Jurassic to Cretaceous (i.e., Harder et al. 2003). The Llangorse volcanic field (LVF) includes Miocene to Holocene volcanic rocks exposed at Hirschfeld Creek, Mt. Sanford, Llangorse Mountain, and Chikoida Mountain (Table 1; Fig. 1). This volcanic field largely overlies Jurassic granodiorite of the Llangorse Mountain Batholith and Cache Creek Group cherts (Aitken 1959) and many of the volcanic occurrences have been described previously (e.g., Nicholls et al. 1982; Higgins and Allen 1985; Carignan et al. 1994; Francis and Ludden 1995). Lavas in the LVF include alkali olivine basalts, basanites, and olivine nephelinites (Fig. 2; Table 2; nomenclature after Francis and Ludden 1990). The Llangorse Mountain locale, a Middle-Pleistocene volcanic remnant, comprises olivine-phyric basanite lava (Fig. 1; Table 1). Other relevant volcanic centres include Table Hill (olivine nephelinite), Lone Point (olivine-nephelinite), and Hidden Ridge (alkali olivine basalt; Figs. 1 and 2; Table 1).

Llangorse Mountain basanite

The focus of this study is the Llangorse Mountain locale which comprises a 100 m thick, 350 m wide bluff of basanite lava situated immediately south of Llangorse Mountain (Fig. 1; Table 1). The lava flow features well-formed, 1–2 m diameter, vertically oriented columnar joints (Fig. 3a,c) and, at its base, the columns fan to define the floor of the paleovalley that was filled by lava (Fig. 3b,d).

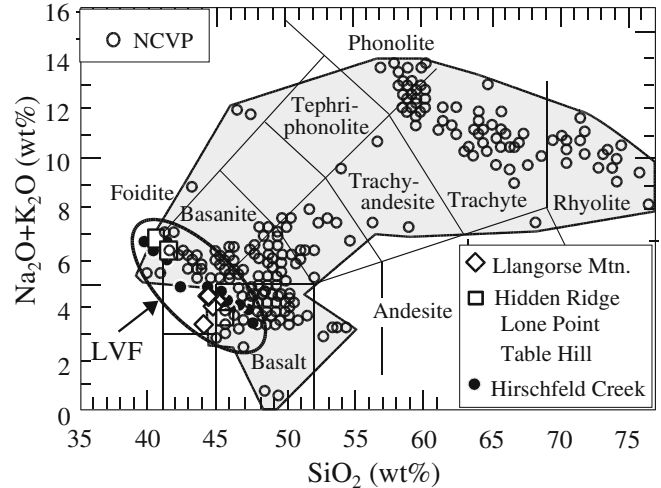


Fig. 2 TAS diagram (Le Bas et al. 1986) comparing chemical compositions of volcanic rocks from the Llangorse volcanic field (LVF) to those of the NCVP (open circles, light-gray shaded region). LVF sites include Llangorse Mountain, Table Hill, Lone Point, Hidden Ridge, and Hirschfeld Creek (see Fig. 1)

The lower margin of the lava flow is also marked by a 30-cm-thick zone of vesicular, quenched basanite. Lava in this basal zone is aphanitic but not glassy (Fig. 4a,c) and is characterized by pervasive, small planar fractures that intersect to form crude polygonal shapes that average

Table 1 Locations and attributes of Miocene to Holocene volcanic rocks in the Llangorse volcanic field

Locality	UTM ^a northing- easting	Rock types ^b	Volcanic landforms represented	Volume (m ³)	Sources ^c
Llangorse Mountain	6582950–625950	Bas, mx > cx	Valley-filling lava flow	2.1×10 ⁷	1, 2, 4, 6, 7
Table Hill	6580122–619838	Ne, mx < cx	Hypabyssal intrusion	3.0×10 ⁶	1, 5, 6, 7
Lone Point	6577850–625600	Ne, mx < cx	Subglacial lava flow	3.0×10 ⁶	1, 5, 6, 7
Hidden Ridge	6585401–628415	Bas, mx cx	Valley-filling lava flow	1.5×10 ⁶	6, 7
Hirschfield Creek	6601100–616900	Ne, Bas, AOB	Hypabyssal intrusion	2.0×10 ⁷	1, 4, 5, 6, 7
Chikoida Mountain	6565200–612450	Bas, cx > mx	Valley-filling lava flow	>1.0×10 ⁶	6, 7
Fire Mountain	6592000–625600	Ne, mx	Dykes	> 5.0×10 ⁴	3, 5, 6, 7

^aNorthing and easting in metres, relative to North American Datum 1927

^bBas Basanite, Ne nephelinite, AOB alkali olivine basalt, mx mantle, cx crustal xenoliths

^c1 Aitken (1959); 2 Nicholls et al. (1982); 3 Higgins and Allen (1985); 4 Carignan et al. (1994); 5 Francis and Ludden (1995); 6 Harder et al. (2003); 7 Edwards et al. (2003)

~0.5–1.0 cm in diameter (Fig 4a). Commonly, small (<1%) amounts of xenocrystic quartz are found in the basanite along the same lower contact.

The basanite lava is fine-grained (200–500 μm), equigranular, contains <5% microphenocrystic olivine and, generally, features a holocrystalline groundmass of plagioclase, clinopyroxene, and olivine, enclosing subordinate amounts of Fe-Ti oxides and nepheline (Fig. 4b). Larger xenocrysts of olivine from disaggregated peridotite xenoliths (see below) are characterized by thin (<50 μm) reaction coronas or resorbed margins. Lava samples from the highly fractured, quenched base of the flow (Fig. 4a) show the same mineralogy as the main bluff, with one important distinction. Primary magmatic biotite (≤2%) is found in all samples collected from the base of the flow (Fig. 4c). It is intergranular and appears as a late-stage crystallization product; the abundance of biotite suggests that higher water contents attended crystallization in the chilled base of the flow.

Crustal (granitic rocks) xenoliths in the basanite are rare (<<1%), small (<1 cm), and appear to derive from the

surrounding Llangorse batholith. The crustal xenoliths may represent surficial material incorporated into the base of the lava during flow, which explains their relatively low abundance and their size.

Mantle-derived xenoliths (spinel-bearing lherzolites and harzburgites) are common at the base of the lava flow (~5 vol%). Most xenoliths are ≤5 cm in size but they commonly range up to 10 cm in size. The largest xenoliths observed were approximately 25–30 cm in diameter. The mantle xenoliths are extremely rare in the upper part of the flow, suggesting one of several possibilities: (1) the entire basanite bluff was molten at one time, allowing the dense xenoliths to settle out of the upper part of the flow and concentrate at the base, or (2) peridotite xenoliths were only present in the early phases of the eruption, or (3) these and other xenoliths are accidental and entrained by the flow during surface transport.

We favour the first suggestion (1) of syn- to post-emplacement sedimentation for several reasons. Firstly, it is unlikely that the mantle xenoliths were incorporated into the base of the flow during surface transport because, other

Table 2 Major element chemical compositions of lavas (MH-02-) from the LVF including replicate (r) analyses of individual samples. Localities include Llangorse Mountain (LM), Lone Point (LP), Table Hill (TH), and Hidden Ridge (HR)

Sample	101	101r	101s	101s	112	160	173	213
Centre	LM	LM	LM	LM	LM	LP	TH	HR
Rock type ^a	Bas	Bas	Bas	Bas	Ne	Ne	Ne	Bas
SiO ₂	45.13	44.99	44.91	45.00	44.11	41.47	40.57	45.57
TiO ₂	2.23	2.21	2.20	2.22	1.92	2.72	2.53	2.05
Al ₂ O ₃	13.12	13.13	13.15	13.18	12.36	11.99	11.70	13.37
Fe ₂ O ₃	2.23	2.59	2.80	2.73	2.63	5.37	6.70	2.76
FeO	10.09	9.68	9.59	9.59	9.76	8.35	7.57	9.58
MnO	0.18	0.18	0.18	0.18	0.18	0.19	0.21	0.19
MgO	11.69	11.61	11.65	11.68	13.55	12.02	10.67	11.04
CaO	9.96	9.96	9.94	9.99	10.24	9.18	9.45	9.37
Na ₂ O	3.14	3.12	3.11	3.15	2.34	4.52	5.22	2.81
K ₂ O	1.23	1.22	1.22	1.22	1.07	1.79	1.76	1.01
P ₂ O ₅	0.50	0.50	0.50	0.51	0.43	1.00	1.30	0.38
Sum	99.51	99.19	99.25	99.45	98.59	98.61	97.68	98.13

^aRock names as in Table 1

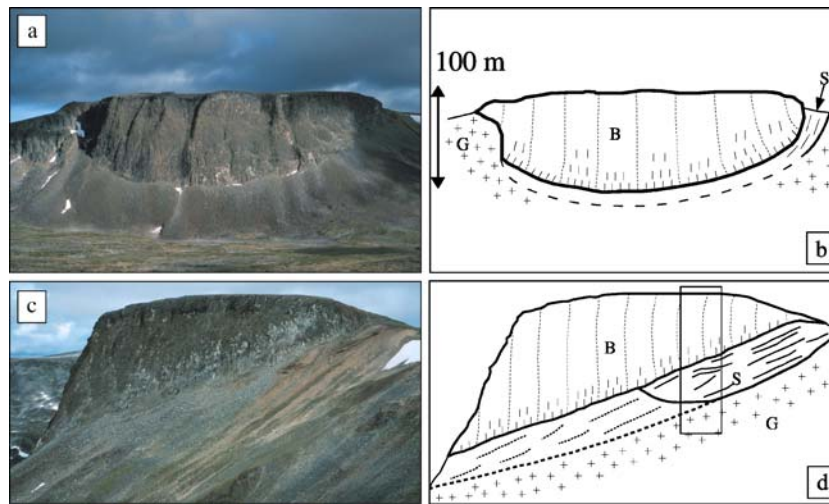


Fig. 3 Field photographs and interpretive sketches of outcrops at the Llangorse Mountain locale. **a** South-facing view of the valley-filling basanite flow. The bluff is approximately 100 m high and 350 m wide. **b** Sketch illustrating contact relationships between the basanite flow (*B*), volcaniclastic sediments (*S*), and granodiorite (*G*), orientation of columnar jointing within basanite flow (*light dashed*

lines) and bedding attitudes in the sediments (*dashed lines*). **c** East-facing view of the basanite flow showing contact against underlying volcaniclastic sediments (*top right corner* of photo). **d** Sketch illustrates contact, bedding, and columnar jointing orientations in **c**. *Vertical rectangle* represents schematic cross-section used in Fig. 7

than the volcanic edifice itself, there is no immediate source of peridotite and they are much more abundant than the crustal xenoliths. Stokes settling velocity calculations (based on a purely Newtonian fluid) suggest that even smaller (5 cm diameter) mantle xenoliths will have settling velocities of ~ 0.01 – 0.1 m/s (cf. Sparks et al. 1977). Such settling velocities are likely to be at least an order of magnitude slower than the rates of eruption. For example, Kauahikaua et al. (2002) estimated eruption rates for the 1800–1801 eruption of olivine-phyric, xenolith-bearing, alkaline basalts from Hualalai volcano to be in excess of 1 m/s. However, the rates of xenolith settling are substantially faster than the time-scales required for transport, emplacement and, especially, cooling of this flow. The implication is that, once erupted, peridotite xenoliths will immediately begin to sediment unless the lava maintains an excessively high stream-bed velocity. It is possible that the earliest phase of the eruption, as represented by the base of the basanite lava flow, was relatively enriched in mantle xenoliths and this could serve to explain the current distribution of xenoliths (e.g., Kauahikaua et al. 2002). However, sedimentation rates for mantle xenoliths in basanite liquid are sufficiently high that, even if evenly dispersed throughout the entire eruption, most (>2 cm) xenoliths would settle to the base of a 100-m-thick flow within tens of hours to days.

Along the western margin of the Llangorse bluff (Fig. 3c,d; Fig. 5a), the basanite lava flow immediately overlies partially lithified, coarse-grained sediments. The contact between lava and underlying sediments appears conformable. There is no evidence of post-depositional erosion or reworking of the sediments, nor is there evidence for weathering or established vegetation on the contact. The same contact is obscured along the eastern side of the massif. There the basanite lava is in contact with

a highly weathered surface of granodiorite belonging to the Llangorse Mountain batholith. The highly weathered nature of the granodiorite at this contact indicates that, at this elevation, the granodiorite was not glaciated. The eastern contact is only exposed near the upper surface of the lava flow and is nearly vertical in orientation. We expect the contact between basanite and sedimentary deposits to lie at lower elevations, where it is obscured by scree sloughed from the lava bluff (Fig. 3a,b). The lack of exposure precludes direct measurement of thickness for the sedimentary deposits, however, based on our observations we suggest a minimum thickness of 45–50 m.

Volcaniclastic sediments

The sedimentary deposits underlying the basanite flow exposed at Llangorse Mountain comprise a sequence of consolidated, but still friable volcaniclastic sediments. The diamictites are very poorly sorted, crudely stratified, matrix-supported, and contain angular to rounded fragments (Fig. 5). The matrix of these sediments has a mean grain size of 1–2.5 mm and there is a distinct lack of silt to clay size fractions. Clasts or fragments vary in size from 1–5 cm to as large as 1–5 m. The stratification or layering is mainly defined by grain-size variations or by pronounced parting surfaces (Fig. 5a,b) and is decimetre scale; less common massive layers are metre scale. In some instances, layering is accentuated by the concentration of large (0.5–1 m) boulders at the top of the bed (Fig. 5b). The stratification is best exposed along the extreme southwest portion of the outcrop (Fig. 3c). There the layering appears primary and dips subparallel to the valley wall at approximately 25° to the northwest.

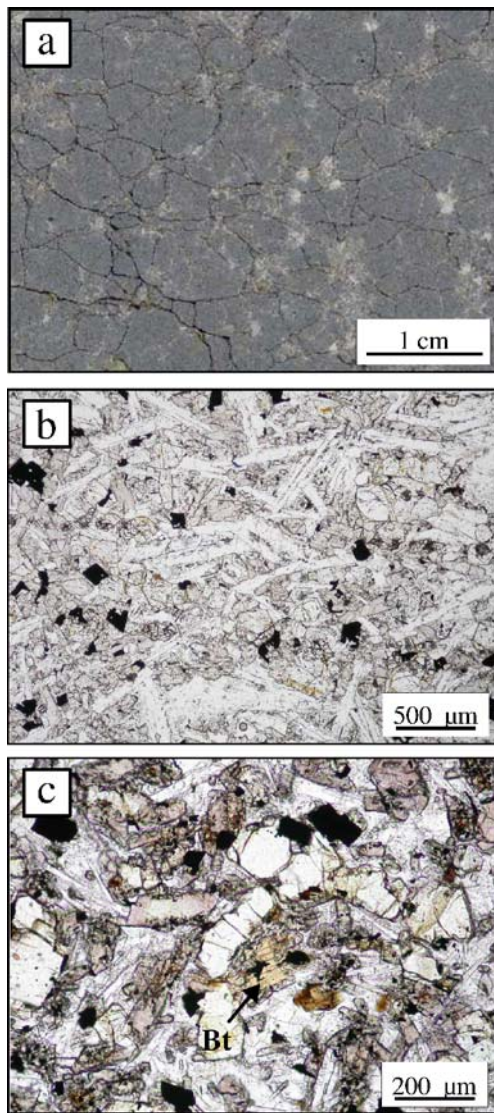


Fig. 4 Textural and petrographic features of basanite lava. **a** Scanned image of polished sample from chilled base of lava flow showing pervasive, irregular polygonal jointing. **b** Photomicrograph of holocrystalline basanite lava. **c** Photomicrograph of basanite from the chilled base of the lava flow overlying volcaniclastic sediments and containing small (<2 vol%) quantities of magmatic biotite (*Bt*)

There are three main types of essential clasts within the diamictites: basanite, granodiorite, and peridotite. These clast types are always present even though their proportions and size distributions vary throughout the section. The matrix to the diamictites is dominated by angular to subangular clasts of basanite, palagonitized basanite and secondary cement. Grains of quartz, feldspar, hornblende and biotite are abundant throughout the matrix (Fig. 6b) and are produced by disaggregation of granodiorite clasts. Olivine, clinopyroxene, and orthopyroxene grains are also common constituents in the matrix and represent fragmented peridotite.

The majority of clasts within the volcaniclastic sediments are fragments of basanite. Most basanite clasts are

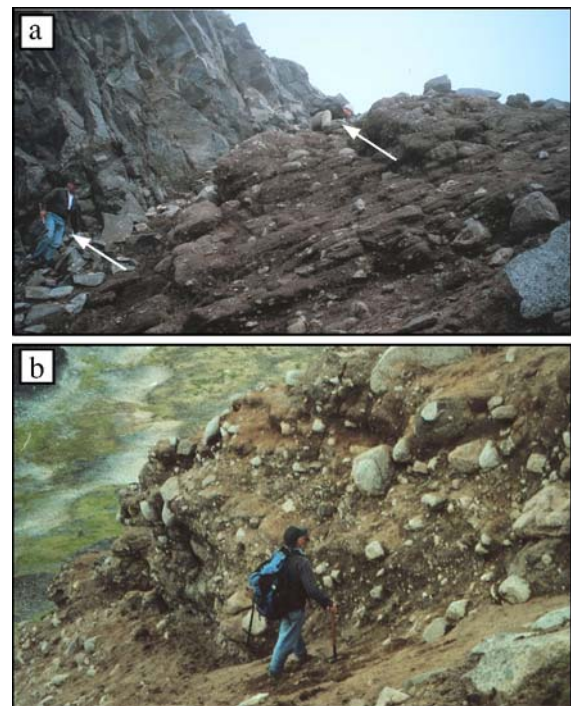


Fig. 5 Field photographs of volcaniclastic sediments underlying basanite lava flow at Llangorse Mountain. **a** Poorly sorted volcaniclastic sediments are characterized by crude decimetre- to metre-scale layering (*arrows* point to people on the sediment/lava contact). **b** Alternate view of volcaniclastic deposits illustrating crudely bedded, poorly sorted, matrix supported, heterolithic nature of sediments. *Light coloured material* comprises rounded blocks of granodiorite

0.5–3 cm in diameter but some layers of diamictite are characterized by fragments of basanite that are up to 50 cm in diameter. Basanite clast types vary from angular to subangular fragments of dense lava (Fig. 6a) to subrounded clasts of vesicular to scoriaceous basanite. Most are vesicular, very fine grained, and commonly contain xenocrysts derived from granodiorite or peridotite xenoliths (Fig. 6b,d). In many instances, the basanite clasts have the well-preserved shapes (fluidal) and textures (stretched vesicles) of primary fragmented pyroclasts (Fig. 6). Fluidal shapes of pyroclasts and the presence of stretched vesicles (e.g., Fig. 6d) are fragile features formed by aerodynamic shaping of low viscosity pyroclasts during eruption and are unlikely to survive high-energy stream sediment transport.

The second most abundant clast type in these diamictites is granodiorite which, on the basis of mineralogy and texture, probably derives from the surrounding Llangorse batholith. Granodiorite clasts comprise 5–20% of these deposits, vary in size from 2 cm to 3 m in diameter (see light coloured blocks in Fig. 5b), and are generally well-rounded. The well-rounded nature of the granodiorite clasts, relative to the angular to subangular volcanic clasts described above, requires a previous history involving relatively well-worked or mature sediments. Glacial-fluvial sediments rich in granodiorite derived from the Llangorse

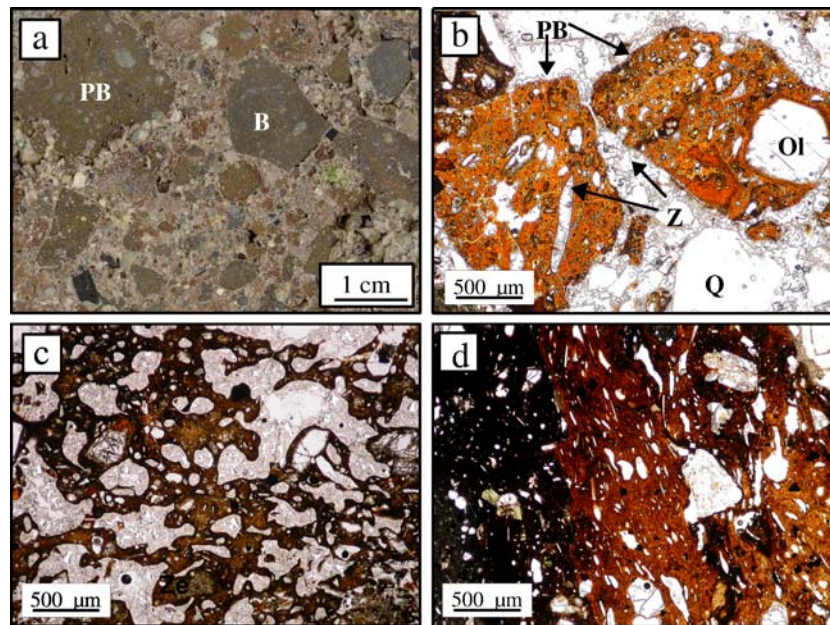


Fig. 6 Detailed textural and petrographic features of volcanoclastic deposits. **a** Scanned image of polished slab of moderately indurated sediments showing angular clasts of basanite lava (*B*) and palagonitized basanite scoria (*PB*) within a finer-grained, poorly sorted, porous clastic matrix. **b** Photomicrograph of palagonitized clasts of vesicular basanite (*PB*) containing olivine (*Ol*) xenocrysts; matrix contains quartz (*Q*), amphibole and biotite grains derived

from the Llangorse batholith. Vesicles and matrix pore space are partly filled by zeolite (*Z*). **c** Palagonitized pyroclast of scoriaceous basanite. **d** Palagonitized pyroclast of basanite showing gradation from a microcrystalline core (*left*) to a rim of palagonitized glass (*right*). Vesicles in the palagonitized rim become increasingly stretched towards the clast boundary

batholith underly much of the present-day landscape, and this is the likely source for the rounded granitoid clasts.

The third essential component to the diamictites is clasts of coarse-grained, mantle-derived peridotite (cf. Harder and Russell 2006). They are a common accessory clast (<3 vol%) and are relatively fragile. They tend to occur as friable, angular to subangular fragments and vary in size from 0.5 cm to a maximum of 25 cm. Some peridotite clasts feature thin coats of aphanitic basanite lava. Conversely, many of the basanite clasts contain small fragments of mantle-derived peridotite xenoliths. Lava flows containing mantle-derived peridotite nodules are reasonably uncommon entities within the NCVP of northern British Columbia (Edwards and Russell 2002). On that basis alone, it seems probable that the xenoliths within the volcanoclastic sediments are closely associated with or related to the xenoliths within the base of the overlying basanite lava flow. Indeed, Harder and Russell (2006) used the peridotite xenoliths to investigate the thermal state of the underlying mantle lithosphere and could find no systematic differences in mineralogy, mineral chemistry or texture between the two populations of xenoliths. Furthermore, the abundant well-preserved pyroclasts of basanite within the diamictites also suggest a strong spatial and temporal connection between deposition of the volcanoclastic deposits and the overlying lava flow.

Many basanite clasts are partially to completely palagonitized (Furnes 1984; Cas and Wright 1987; Thorseth et al. 1991; Stroncik and Schmincke 2002) and now are composed of a fine-grained mixture of clays dom-

inated by smectite. Palagonitized basanite clasts can comprise up to 30% of the volcanoclastic sediment (Fig. 6a,b) and vary in appearance from a bright orange, transparent material to a dark red-brown, nearly opaque material (Fig. 6). In some larger clasts, 1–2 cm thick rinds of palagonite encompass aphanitic, microcrystalline cores of basanite (Fig. 6d). Palagonitized clasts vary in vesicularity from 5 to 55% (e.g., Fig. 6c) and, in all clasts, primary porosity (vesicles) is partly to completely filled by secondary zeolite (mainly chabazite) cements (Fig. 6b). In the highly palagonitized portions of the deposit, zeolite coats most clasts and fills in pore space in the matrix, causing lithification of the diamictite.

Discussion

Syngenetic debris flows

A debris flow origin for the diamictite deposits underlying the basanite flow is supported by the poorly sorted, matrix-supported, and crudely bedded character of the sediments (e.g., Cas and Wright 1987; Geirsdottir 1990; McPhie et al. 1993). Such an origin is also strongly indicated by the size distribution of clasts and the diversity in composition and shape of clasts. The lack of clay to silt size fractions in the matrix suggests a juvenile unweathered source such as would be found on the slopes of an active volcanic edifice. Grain size distributions vary substantially between layers but the sediments commonly contain centimetre, deci-

metre, and metre-scale lithic blocks (e.g., up to 3–5 m). These clasts derive from two distinct sources and have substantially different shapes. The diamictite deposits juxtapose well-rounded granodiorite clasts derived from pre-existing glacio-fluvial sediments against angular to fluidal-shaped juvenile pyroclasts of basanite from a primary volcanic source.

The crudely stratified character of the debris flow deposits (Fig. 5a) could result from several disparate processes. The debris flow deposits may have been deposited *en masse*, in which case the layering might be a manifestation of shearing at the base of the flow causing sedimentation and some sorting (e.g., Cas and Wright 1987; McPhie et al. 1993). Alternatively, the mass flows may have been assembled progressively (Branney and Kokelaar 1992; McPhie et al. 1993) but with fluctuating rates of aggradation to account for the variations in the scales of stratification (e.g., decimetre to metre). Lastly, the diamictites may represent multiple episodes or pulses of debris flow sedimentation. In this case, there would have been little to no hiatus between the mass flow events because there is no evidence of fluvial reworking or more dilute sedimentation at the tops of the individual layers (e.g., fine-scale lamination, graded bedding, cross-bedding). The attributes of these deposits are consistent with high-energy flood events producing water-saturated debris flows over short (hours to days) periods of time (e.g., Björnsson 1975; Geirsdottir 1990; Knighton 1998; Vallance 2000).

A syngenetic relationship between the basanite lava and the underlying debris flow deposits is indicated by the composition and character of the clasts within the sediment. Most Neogene lavas in the NCVP are alkali-olivine basalt in composition and occurrences of basanite lava are relatively rare (Edwards and Russell 2002). The basanite clasts in the sediments are petrographically (e.g., mineralogy, texture) equivalent to the overlying basanite lava. As discussed above, peridotite clasts from the sediments and peridotite xenoliths from the lava flow show no discernible mineralogical or chemical differences, and appear to represent the same mantle source region (Harder and Russell 2006). Therefore, we suggest that there is a single source of peridotite-bearing basanite and that this source supported the production of volcanoclastic debris flows as well as lava flows.

The apparently conformable contact between the debris flow sediments and the lava further suggests that deposition of the debris flows and emplacement of the lava flow were closely related in time. The highly fractured nature of the base of the overlying lava flow (Fig. 4a) is similar to the small-scale, chaotic columnar or cube jointing found in water or ice quenched lavas (e.g., Grossenbacher and McDuffie 1995; Lescinsky and Fink 2000). This type of jointing is interpreted to result from steam generation that disrupts isotherms during cooling (Lescinsky and Fink 2000). At the Llangorse locale, therefore, this jointing pattern may indicate that the lava flow was quenched against the underlying water-saturated sediments. Higher water contents in the base of the lava flow are also

indicated by the presence of primary magmatic biotite (Fig. 4c) and may have resulted from mixing of the underlying, wet debris flow sediments into the basal portion of the lava (e.g., Zimanowski and Büttner 2002). This mechanical mixing between the unconsolidated sediments and overlying basanite could also account for the presence of small amounts of granitic material (e.g., quartz xenocrysts) concentrated at the base of the flow.

The debris flow sediments have many features indicative of their source region and transport distance. Firstly, the sediments have an immature matrix, with few clay and silt-sized particles. Secondly, a high proportion of basanite clasts are fluidal-shaped or highly vesicular, and clasts of peridotite are common. These fragile juvenile volcanic features and friable peridotite clasts are rapidly destroyed or disaggregated by transport. The high proportion of volcanic material in the sediments further indicates that the sediments sourced near the volcanic vent. In particular, the abundance of glassy basanite clasts (now palagonitized) indicates that the debris flows sampled material on or near the volcanic edifice and supports a proximal, volcanic source to the debris flows.

Debris flows are commonly associated with volcanic eruptions (e.g., lahars, outburst floods) because of the highly unstable and friable nature of juvenile volcanic material and steep topography often found in volcanic landscapes (Björnsson 1975; Cas and Wright 1987; Geirsdottir 1990; Vallance 2000). Our interpretation of these debris flows, as lahars that are syngenetic with the lava flow, suggests the production and release of substantial volumes of water in association with the volcanic eruption. A possible source for this water is the melting of a snow pack or glacial ice covering the vent. The high concentrations of juvenile materials in the lahars support the suggestion that the volcanic fragmentation event(s) were actually coincident with melt water generation. Such events could include lava fountaining onto the snow and ice, or lava flow collapse on snow and ice leading to generation of block and ash flows and debris flow torrents (e.g., Thouret 1990; Smellie 2002). Continued eruption led to the production of a basanite lava flow, which was captured by the same drainage used by the debris flows.

In-situ palagonitization

An unusual aspect of the debris flow sediments is the presence of palagonitized clasts of basanite. Palagonitized glass forms via the hydration and breakdown of volcanic glass (usually basaltic) in water-saturated environments, and is a common feature of hyaloclastite deposits (Cas and Wright 1987; Stroncik and Schmincke 2002). Palagonitization is most commonly found in subaqueous (submarine or subglacial) deposits (e.g., Cas and Wright 1987; Stroncik and Schmincke 2002; Thorseth et al. 1991; Furnes 1984) or in deposits subjected to hydrothermal circulation of fluids (e.g., Jakobsson 1978; Jakobsson and Moore 1986). Early workers demonstrated that minimum

temperatures of 50–100°C are generally required for palagonitization to occur on time-scales of less than 1,000 years (Friedman and Smith 1960; Moore 1966).

Only high-temperature palagonitization processes produce smectite clays such as those found in the palagonitized basanite clasts at the Llangorse locale (Schiffman et al. 2002). Subaerial deposits that are subjected only to weathering do not undergo palagonitization, but produce a completely different suite of clay and zeolite minerals (Schiffman et al. 2000, 2002). Higher fluid temperatures (>100°C) are also conducive to the formation of authigenic zeolite cements (Schiffman et al. 2000, 2002). Thus, the pervasive distribution of smectite clay and zeolite cementation in the lahars from Llangorse Mountain supports a higher-temperature origin for the palagonitized basanite clasts. Further support for elevated fluid temperatures in these deposits is found in the colour of palagonitized glass. Dark-brown to red-brown palagonite is associated with higher temperature fluids (80–120°C) than orange palagonite (Stroncik and Schmincke 2001, 2002). Thus, the widespread distribution of dark-brown to red-brown palagonite in these debris flow sediments (Fig. 7d,f) suggests fluid temperatures in excess of 80°C. If the lahars derived from melting of snow or ice, they were probably warm (20–40°C) at the time of deposition (Vallance 2000). Regardless of the initial temperature of the debris flow sediments, the contemporaneous overlying basanite flow provided an efficient vehicle for heating the underlying water-saturated deposits (Fig. 7). We suggest this process led to hydrothermal, in-situ palagonitization of the glassy basanitic clasts in the sediments.

We have tested this concept by modeling the heating of the subsurface by the basanite lava flow (Fig. 7). The model also constrains the possible distribution (depth) and timing of palagonite formation. We use a one-dimensional, transient, heat conduction model to simulate the cooling history of the basanite lava flow and the heating and cooling history of the subsurface (e.g., Carslaw and Jaeger 1959; Philpotts 1990). The lava is given a thickness of 60 m (an average value to account for the wedge-shaped flow morphology) and is assumed to have a single uniform emplacement temperature (1,200°C). The upper surface of the lava cools to the atmosphere via natural convection and the base conducts heat to the ground which maintains a far-field temperature of 10°C. The upper boundary condition causes the upper surface of the lava to cool to solidus temperatures and potentially form a crust in a few hours; this allows the effects of radiative heat loss to be ignored. Potential heat sources and sinks for the lava and the underlying stratigraphy were considered. However, our calculations showed that the heats of crystallization within the lava are easily balanced by the heats attending phase changes in the subsurface (e.g., steam production and mineral transformations). On this basis and following the work of others (e.g., Patino-Douce et al. 1990), we elected not to include heat sources or sinks. The pore water in the sediments is heated but the model does not allow for convection. The last simplifying assumption is that the bulk physical properties (e.g., thermal diffusivity) assigned

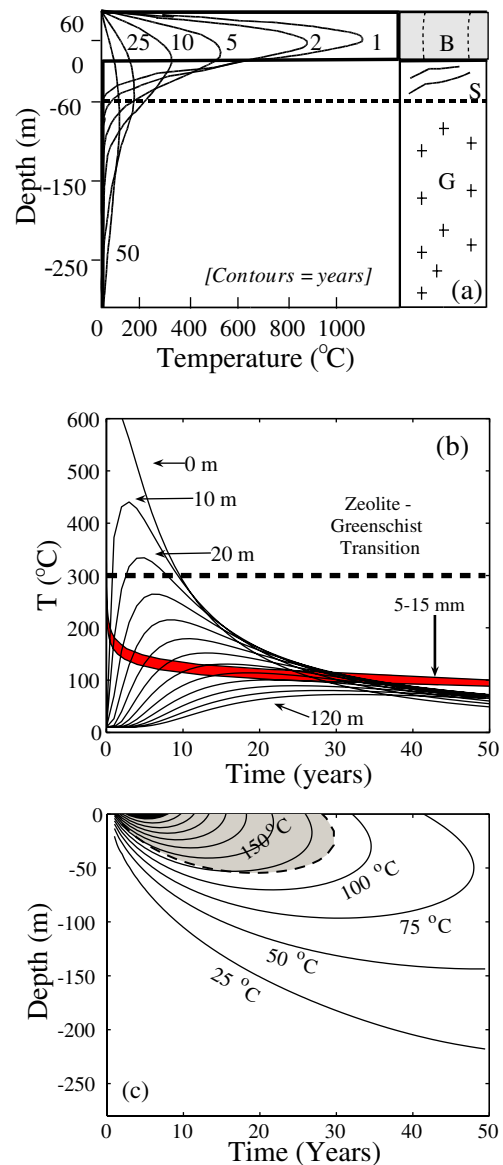


Fig. 7 Model heating and cooling history of volcanoclastic deposits underlying basanite lava flow. **a** Model results summarized as temperature–depth curves at specific times (years) showing relationship between cooling of 60-m-thick basanite lava (*B*) and heating of subsurface sediments (*S*) and granodiorite (*G*). **b** Temperature–time curves for heating and cooling of the subsurface based on depth (e.g., 0, 10, 20 ... 120 m) below the basanite-sediment contact. Conditions for palagonite formation are met where the heating–cooling curves intersect the minimum conditions ($T^{\circ}\text{C}$ - time) required to produce palagonite rind thicknesses of 5–15 mm (*heavy curve*). The high temperature limit to zeolite facies is also shown. **c** The 'palagonite window' (*shaded field*) resulting from heating of sediments by the overlying basanite flow is mapped in depth (m) vs. time space. *Solid lines* are isotherms ($^{\circ}\text{C}$) showing the heating–cooling history of the subsurface

to the lava flow and underlying fluid saturated sediments are assumed to be constant and independent of temperature. The boundary value problem was solved by finite-difference using fixed step sizes.

The transient temperature distribution in the lava flow and the subsurface are shown for a series of specific times

in Fig. 7a. The lava flow cools to $<200^{\circ}\text{C}$ within 25 years, while the subsurface (up to 50 m below the contact) is heated to 100°C and is maintained at that temperature for 25 years (Fig. 7a,b). The contact is heated to approximately half the temperature of the lava flow (i.e., $\sim 600^{\circ}\text{C}$) and maintained at temperatures $>100^{\circ}\text{C}$ for close to 50 years. At 20 m below the contact, the ground is gradually heated to temperatures in excess of 300°C but cools back to ambient conditions after 50 years. These heating and cooling curves for the subsurface (Fig. 7b) can be used to explore where, in depth and time, they intersect the conditions required for palagonitization of the debris flow sediments (Moore 1966; Friedman and Smith 1960; Schiffman et al. 2000, 2002; Stroncik and Schmincke 2002).

No primary basanite glass remains in the debris flow deposits due to extensive palagonitization, which makes it difficult to estimate the maximum extent of palagonitization. There are, however, basanite clasts that exhibit palagonitized rims surrounding microcrystalline cores (Fig. 6f); the thickness of these palagonitized rims provides a minimum estimate of the extent of palagonitization. In Fig. 7b, we compare the model heating–cooling curves for specific depths in the subsurface (solid lines; 0, 10, 20 m) to the temperature–time conditions (shaded curve) required to generate palagonite rim thicknesses of between 5 and 15 mm using the most recent rate laws (e.g., Techer et al. 2001; Stroncik and Schmincke 2002). Palagonitization is predicted when the individual heating–cooling curves pierce this shaded curve. The upper temperature limits of palagonite formation coincide roughly with the transition from zeolite to greenschist facies metamorphism (300°C ; Fig. 7b; Stroncik and Schmincke 2002). Thus, some paths preclude the formation of palagonite because the heating path converts all palagonite and glass to higher temperature mineral assemblages which will be preserved or altered to other low-temperature assemblages (e.g., non-palagonite) depending on the rates of cooling.

These results lead to the concept of a ‘palagonite window’ mapped in Fig. 7c. the palagonite window is defined by the intersections of the model heating–cooling curves (Fig. 7a,b) with the critical $T(^{\circ}\text{C})$ - t conditions for formation of 5–15 mm rims of palagonite (Fig. 7b). This window (grey shaded field; Fig. 7c) shows the maximum depths and times for palagonitization of the subsurface deposits compared to the isotherms (solid lines) predicted for the subsurface deposits. The isotherms illustrate the maximum amount of subsurface heating and the critical times where the subsurface begins cooling (Fig. 7c). For example, the 100°C isotherm obtains a maximum depth of 70 m, but after 35 years, the entire subsurface has cooled to temperatures below 100°C .

This simple model shows that the basanite lava flow at Llangorse Mountain had the capacity to heat the underlying debris flow sediments to temperatures of 100 – 125°C . The model palagonite window suggests that this process would allow for formation of 5–15 mm rims of palagonite on glassy clasts in material up to 50 m below the contact and would be complete within 30 years. Beyond these depth

and time limits, the temperatures of pore fluids would be too low for efficient palagonite formation.

Glaciovolcanism in the LVF

The valley-filling basanite lava flow exposed at Llangorse Mountain (100 m thick, 350 m wide; Fig. 3a) has an aspect ratio (flow thickness/flow width) of approximately 0.3; low viscosity basanite lavas typically form sheet like bodies with aspect ratios on the order of 10^{-4} (e.g., Reidel 1998). Clearly, the Llangorse Mountain bluff is overthickened by ~ 3 orders of magnitude. Moreover, the upper surface of the lava is horizontal despite the 25° dip of the paleovalley floor, giving the lava a wedge-shaped cross-sectional profile (Fig. 3c,d). The wedge-shaped morphology and the overthickened aspect ratio of these lavas indicates that the lava ponded against a lower-elevation, valley-wide barrier.

The present day valley below the Llangorse Mountain bluff is a wide, glacially sculpted U-shaped valley that offers no current physical barrier. Large sheets of glacial ice filling this valley at lower elevations would provide a likely barrier against which the lava ponded (Fig. 8; e.g., Mathews 1951, 1952). This association of volcanic eruption with glaciation is typical of the NCVF, where there is abundant evidence of synglacial and subglacial volcanism reflecting the coincidence of Pliocene to Pleistocene glaciers with volcanism (Edwards and Russell 2000). For example, the Tuya-Teslin volcanic district contains numerous subglacial volcanic edifices, including the type locality for tuyas (Mathews 1947; Edwards and Russell 2002).

Evidence for glaciovolcanism is also preserved at several other volcanic localities in the LVF. The first is the Lone Point locality (Fig. 1; Table 1) where a 200-m-diameter-mound-shaped outcrop of nephelinite is exposed. The Lone Point outcrop shows a complex pattern of columnar jointing, characterized by well-developed, 10–30 cm diameter columns with highly variable (i.e., fanning) orientations. The second of these localities is Hidden Ridge (Table 1; Fig. 1) which features a ridge of basanite approximately 250×100 m in area. In overall morphology, Hidden Ridge is very similar to the Llangorse Mountain bluff. The Hidden Ridge basanite is a valley-filling lava flow that overlies a sequence of coarse, poorly sorted, crudely bedded debris flow deposits containing clasts of granodiorite, basanite lava, and peridotite. The geographic proximity and numerous similarities between Hidden Ridge and the Llangorse locale suggest that the two localities are roughly coeval in age and may have sourced from the same volcanic vent. Hidden Ridge also displays variably oriented columnar joints, similar to Lone Point. Erratic size and orientations of columnar jointing in lavas at Lone Point and Hidden Ridge require both vertical and horizontal cooling surfaces to explain the jointing patterns. Strong variations in size and orientation of cooling joints are also often indicative of interactions between lava and ice masses (e.g., Mathews 1947; Jones 1966, 1969; Grossenbacher and McDuffie 1995; Lescinsky and Fink 2000; Edwards et al. 2002; Kelman et al. 2002), suggesting

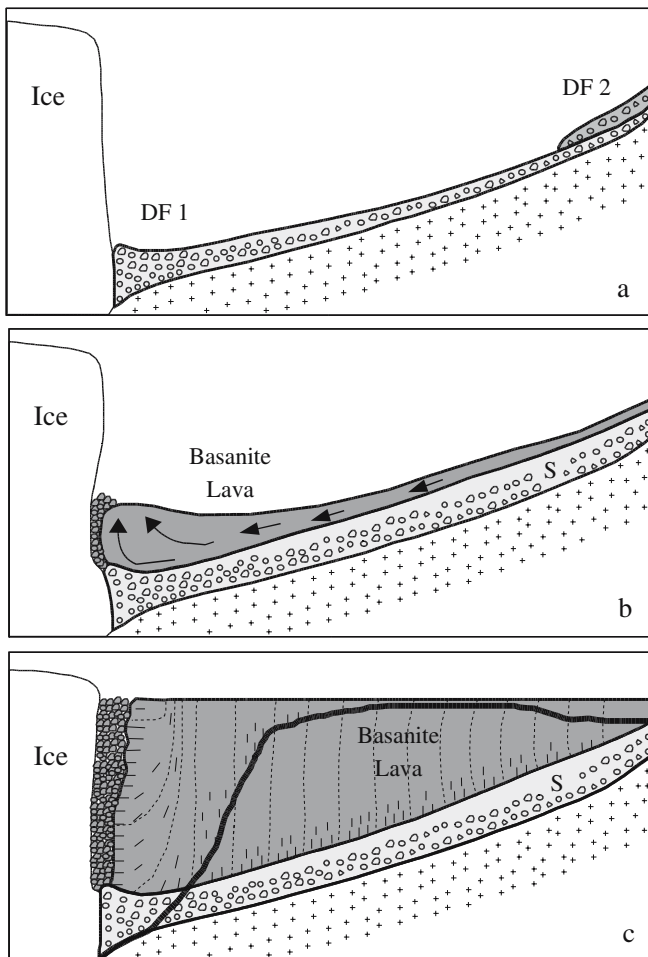


Fig. 8 Interpretive sketch of the impoundment of the debris flow sediments and basanite lava at Llangorse Mountain locale (vertical exaggeration $>15\times$). **a** Early stages of eruption produce a sequence of debris flows (*DF1*, *DF2*, ...) ponding against glacial ice. **b** Subsequent lava flow is captured by the same drainage system, overrides debris flow sediments, and is impounded against ice, causing inflation and overthickening (*see arrows*) at the flow front. **c** Final post-eruption configuration includes a large overthickened mass of basanite lava; lava-ice interface is marked by accumulated rubble (*see text*). *Light dashed lines* trace the orientations of columnar jointing within the flow. Present-day exposure of the basanite flow and debris flow sediments denoted by *heavy solid line* (Fig. 3d is corresponding field photo)

that lavas at these localities were erupted under or against glacial ice.

Volcanological model for Llangorse mountain

The relative sequence of events producing the stratigraphic relationships observed at Llangorse Mountain are schematically illustrated in Fig. 8. The paleo-landscape consists of pre-existing drainage systems cut into granodiorite bedrock and leading to glacial ice sheets present at lower-elevation regions. The first stage of the eruption sequence (Fig. 8a) features contemporaneous production of large volumes of water from melting of snow or ice by the eruption of

basanite. Release of this melt water generated lahars which traveled down-valley, ultimately abutting and piling up against glacial ice. Portions of this drainage system may well have comprised tunnels and tubes within a large ice sheet.

The basanite lava flow used the same drainage systems and overrode the lahars shortly after they were deposited (Fig. 8b). The lava ponded against the valley glacier and continued flow resulted in inflation of the lava flow at its terminus (Fig. 8b; e.g., Cashman et al. 1998), ultimately producing a 100-m-thick flow front (Fig. 8c). The ice-lava interface probably featured rubble that accumulated from the collapse of the pervasive, fine-scale, columnar to cube jointed flow fronts that characteristically develop in ice-contact (quenched) lava masses (e.g., Mathews 1952; Lecinsky and Fink 2000; Edwards et al. 2002; Edwards and Russell 2002). The outer margins of the coherent lava flow would feature horizontal platy jointing, grading into polygonal, small-scale jointing, and ultimately into the large (metre-scale), vertical columnar joints observed today in the centre of the lava flow (Fig. 8c). The present-day vertical lava bluff (dark solid line; Fig. 8c) lacks any trace of horizontal columnar jointing, suggesting that the leading edge of the lava flow has been removed. We suggest that as the glacier receded, the highly unstable and over-steepened front of the lava flow collapsed. Mass wasting of the front of the overthickened, cliff-forming lava flow continues, forming a large apron of scree composed of blocks of columnar-jointed basanite, which surrounds the lava bluff and in most areas obscures the lower contact of the lava flow.

Conclusions

The Llangorse volcanic field, in northwestern BC, comprises Miocene-Holocene mafic, alkaline lavas. The focus of this study is a large, Middle Pleistocene, valley-filling basanite lava flow exposed south of Llangorse Mountain. We interpret debris flow sediments underlying the lava flow as syngenetic lahars or outburst floods that sourced from melting of a snow-pack or glacier around the volcanic vent in the early stages of eruption. Volcanic material was sampled near the vent and transported downslope in high-energy debris torrents. An effusive basanite lava flow soon followed the debris flows; the lava ultimately entered a drainage system blocked at lower elevations by valley-filling glaciers, causing the flow to pond and overthicken to at least 100 m. Emplacement of the lava flow induced hydrothermal circulation of fluids in the underlying, water-saturated debris flow and resulted in in-situ palagonitization of the glassy pyroclasts of basanite. This rapid, high temperature (80–100°C) palagonitization also produced authigenic zeolite cements which partly indurated the debris flow sediments. Our simple thermal model shows that the basanite flow heated the underlying ground (debris flow sediments and granodiorite country rock) to temperatures in excess of 100°C and maintained these temperatures for up to 50 years. Lastly, on the basis of thermal models and experimentally determined rates of

palagonitization, we develop a 'palagonite window' which maps the depth (50 m)/time (30 years) limits for in-situ palagonitization of basanite clasts within the Llangorse Mountain debris flow sediments.

Acknowledgements Field costs for this study were covered by the Geological Survey of Canada, courtesy of the Atlin Integrated Geoscience Project (R.G. Anderson). All other costs were met through NSERC via a Discovery Grant to J.K. Russell and a PGS-A scholarship to Margaret Harder. Our research benefited from discussions with Kirstie Simpson, Ian Skilling and Ben Edwards, and the manuscript was improved substantially via critical and thoughtful reviews by Dave Lescinsky and an anonymous reader.

References

- Aitken JD (1959) Atlin, British Columbia. *Geol Surv Can Mem* 307
- Björnsson H (1975) Subglacial water reservoirs, jökulhlaups and volcanic eruptions. *Jökull* 25:1–11
- Branney MJ, Kokelaar P (1992) A reappraisal of ignimbrite emplacement: progressive aggradation and changes from particulate to non-particulate flow during emplacement of high-grade ignimbrite. *Bull Volcanol* 54:504–520
- Carignan J, Ludden J, Francis D (1994) Isotopic characteristics of mantle sources for quaternary continental alkaline magmas in the northern Canadian Cordillera. *Earth Planet Sci Lett* 128:271–286
- Carslaw HS, Jaeger JC (1959) *Conduction of heat in solids*, 2nd edn. Clarendon Press, New York
- Cas RAF, Wright JV (1987) *Volcanic successions, modern and ancient*. Chapman and Hall, New York
- Cashman K, Pinkerton H, Stephenson J (1998) Introduction to special section: Long lava flows. *J Geophys Res* 103:27, 281–27, 289
- Edwards BR, Russell JK (2000) Distribution, nature, and origin of Neogene-quaternary magmatism in the northern Cordilleran volcanic province, Canada. *Geol Soc Amer Bull* 112:1280–1295
- Edwards BR, Russell JK (2002) Glacial influences on morphology and eruptive products of Hoodoo Mountain volcano, Canada. In: Smellie JL, Chapman MG (eds) *Volcano-ice interaction on earth and mars*. *Geol Soc Lond Spec Pub* 202:179–194
- Edwards BR, Russell JK, Anderson RG (2002) Subglacial, phonolitic volcanism at Hoodoo Mountain volcano, northern Canadian Cordillera. *Bull Volcanol* 64:254–272
- Edwards BR, Russell JK, Harder M (2003) An overview of Neogene to Recent Volcanism in the Atlin volcanic district of the northern Cordilleran volcanic province, northwestern British Columbia. *Geol Surv Can Curr Res* 2003–A08
- Francis D, Ludden J (1990) The mantle source for olivine nephelinite, basanite, and alkaline olivine basalt at Fort Selkirk, Yukon, Canada. *J Petrol* 31:371–400
- Francis D, Ludden J (1995) The signature of amphibole in mafic alkaline lavas, and study in the northern Canadian Cordillera. *J Petrol* 36:1171–1191
- Friedman II, Smith RL (1960) A new dating method using obsidian, part 1: the development of the method. *Amer Antiquity* 25:476–522
- Furnes H (1984) Chemical changes during progressive subaerial palagonitization of a subglacial olivine tholeiite hyaloclastite: a microprobe study. *Chem Geol* 43:271–285
- Geirsdottir A (1990) Diamictites of late Pliocene age in western Iceland. *Jökull* 40:3–26
- Grossenbacher KA, McDuffie SM (1995) Conductive cooling of lava: columnar joint diameter and stria width as functions of cooling rate and thermal gradient. *J Volcanol Geotherm Res* 69:95–103
- Harder M, Russell JK (2006) Thermal state of the mantle lithosphere beneath the Northern Cordilleran Volcanic Province, British Columbia. *Lithos* 87:1–22
- Harder M, Russell JK, Anderson RG, Edwards BR (2003) Llangorse volcanic field, British Columbia. *Geol Surv Can, Curr Res* 2003–A6
- Higgins MD, Allen JM (1985) A new locality for primary xenolith-bearing nephelinites in northwestern British Columbia. *Can J Earth Sci* 22:1556–1559
- Jakobsson SP (1978) Environmental factors controlling the palagonitization of the Surtsey tephra, Iceland. *Geol Soc Denmark Bull* 27:91–105
- Jakobsson SP, Moore JG (1986) Hydrothermal minerals and alteration rates at Surtsey volcano, Iceland. *Geol Soc Amer Bull* 97:648–659
- Jones JG (1966) Intraglacial volcanoes of southwest Iceland and their significance in the interpretation of the form of the marine basaltic volcanoes. *Nature* 212:586–588
- Jones JG (1969) Intraglacial volcanoes of the Laugarvatn region, southwest Iceland. *I. Q J Geol Soc Lond* 124:197–211
- Kauhikaua J, Cashman K, Clague D, Champion DJ, Hagstrum J (2002) Emplacement of the most recent lava flows on Hualālai Volcano, Hawai'i. *Bull Volcanol* 64:229–253
- Kelman M, Russell JK, Hickson CJ (2002) Effusive intermediate glaciovolcanism in the Garibaldi Volcanic Belt, southwestern British Columbia, Canada. In: Smellie JL and Chapman MG (eds) *Volcano-ice interaction on earth and mars*. *Geol Soc Lond Spec Pub* 202:195–211
- Knighton D (1998) *Fluvial forms and processes, a new perspective*. Oxford University Press, London
- Le Bas MJ, Le Maitre RW, Streckeisen A, Zanettin B (1986) A chemical classification of volcanic rocks based on the total alkali-silica diagram. *J Petrol* 27:745–750
- Lescinsky DT, Fink JH (2000) Lava and ice interaction at stratovolcanoes: Use of characteristic features to determine past glacial events and future volcanic hazards. *J Geophys Res* 105:23711–23726
- Mathews WH (1947) 'Tuyas', flat-topped volcanoes in northern British Columbia. *Amer J Sci* 245:560–570
- Mathews WH (1951) The table, a flat-topped volcano in southern British Columbia. *Amer J Sci* 249:830–841
- Mathews WH (1952) Ice-dammed lavas from Clinker Mountain, southwest British Columbia. *Amer J Sci* 250:553–565
- McPhie J, Doyle M, Allen R (1993) *Volcanic textures: a guide to the interpretation of textures in volcanic rocks*. CODES University of Tasmania, Hobart
- Moore JG (1966) Rate of palagonitization of submarine basalt adjacent to Hawaii. *US Geol Surv Prof Paper* 550-D:D163–D171, USGS, Reston, VA
- Nicholls J, Stout MZ, Fiesinger DW (1982) Petrologic variations in quaternary volcanic rocks, British Columbia, and the nature of the underlying upper mantle. *Contrib Mineral Petrol* 79:201–218
- Patino-Douce AE, Humphreys ED, Johnston AD (1990) Anatexis and metamorphism in tectonically thickened continental crust exemplified by the Sevier hinterland, western North America. *Earth Planet Sci Lett* 97: 290–315
- Philpotts AR (1990) *Principles of igneous and metamorphic petrology*. Prentice Hall, Englewood Cliffs, New Jersey
- Reidel SP (1998) Emplacement of Columbia River flood basalt. *J Geophys Res* 103:27, 393–27, 410
- Schiffman P, Spero HJ, Southard RJ, Swanson DA (2000) Controls on palagonitization versus pedogenic weathering of basaltic tephra: Evidence from the consolidation and geochemistry of the Keanakako'i Ash Member, Kilauea Volcano. *Geochem Geophys Geosyst* 1(8). DOI 10.1029/2000GC000068
- Schiffman P, Southard RJ, Eberl DD, Bishop JL (2002) Distinguishing palagonitization from pedogenically-altered basaltic Hawaiian tephra: mineralogical and geochemical criteria. In: Smellie JL, Chapman MG (eds) *Volcano-ice interaction on earth and mars*. *Geol Soc Lond Spec Pub* 202:393–405

- Smellie JL (2002) The 1969 subglacial eruption on Deception Island (Antarctica): events and processes during an eruption beneath a thin glacier and implications for volcanic hazards. In: Smellie JL, Chapman MG (eds) *Volcano-ice interaction on earth and mars*. Geol Soc Lond Spec Pub 202:59–79
- Sparks RS, Pinkerton H, MacDonald R (1977) The transport of xenoliths in magmas. *Earth Planet Sci Lett* 35:234–238
- Stroncik NA, Schmincke H-U (2001) Evolution of palagonite: Crystallization, chemical changes, and element budget. *Geochim Geophys Geosystems* 2: DOI 10.1029/2000GC000102
- Stroncik NA, Schmincke H-U (2002) Palagonite: a review. *Int J Earth Sci* 91:680–697
- Techer I, Advocat T, Lancelott J, Liotard J-M (2001) Dissolution kinetics of basaltic glasses: control by solution chemistry and protective effect of the alteration film. *Chem Geol* 176:235–263
- Thorseth IH, Furnes H, Tumyr O (1991) A textural and chemical study of Icelandic palagonite of varied composition and its bearing on the mechanism of the glass-palagonite transformation. *Geochim Cosmochim Acta* 55:845–850
- Thouret J-C (1990) Effects of the November 13, 1985 eruption on the snow pack and ice cap of Nevado del Ruiz Volcano, Colombia. In: Williams SN (ed) *Nevado del Ruiz Volcano, Colombia I*. *J Volcanol Geotherm Res* 41:177–201
- Vallance JW (2000) Lahars. In: *Encyclopedia of volcanoes*. Academic Press, San Diego, pp 601–616
- Zimanowski B, Büttner R (2002) Dynamic mingling of magma and liquefied sediments. *J Volcanol Geotherm Res* 114:37–44